Chapter 8
Mercury Emissions from Global Biomass Burning: Spatial and Temporal Distribution

Hans. R. Friedli, Avelino F. Arellano, Jr., Sergio Cinnirella, and Nicola Pirrone

Summary This chapter represents a new addition to the UNEP global mercury budget: the mercury emissions from biomass burning, here defined as emissions from wildfires and prescribed burns, and excluding contributions from bio-fuel consumption and charcoal production and use. The results cover the 1997-2006 timeframe. The average annual global mercury emission estimate from biomass burning for 1997-2006 is 675 ± 240 Mg yr^{-1}. This accounts for 8% of all current anthropogenic and natural emissions. The largest Hg emissions are from tropical and boreal Asia, followed by Africa and South America. They do not coincide with the largest carbon biomass burning emissions, which originate from Africa. Our methodology for budget estimation is based on a satellite-constrained bottom-up global carbon fire emission database (GFED version 2), which divides the globe into regions with similar ecosystems and burn behaviour. To estimate mercury emissions, the carbon model output is paired with regional emission factors for Hg, EF(Hg). There are large uncertainties in the budget estimation associated with burned area, fuel mass, and combustion completeness. The discrepancy between the model and traditional ground based assessments (e.g. FRA, 2000) is unacceptably large at this time. Of great urgency is the development and validation of a model for mercury cycling in forests, accounting for the biogeochemistry for each region. This would provide an understanding of the source/sink relationship and thus mercury accumulation or loss in ecosystems. Limiting the burning of tropical and boreal forests would have two beneficial effects: reducing the source of mercury releases to the atmosphere from burning, and maintaining a sink for atmospheric mercury. Restricting the global release mercury would reduce the vegetation/soil pools, and the potential Hg release in case of fire.

8.1 Introduction

The importance of mercury emissions to the atmosphere from biomass burning was first recognized in South America by Veiga et al. (1994), probably as the result of the confluence of mercury pollution from artisan gold mining and ongoing clearing of tropical forests by burning for agricultural uses. After 2000, research describing

laboratory and field experiments extended to other geographic regions with extensive wildfire activity. The concern for this newly recognized pathway of mercury is about its participation in the biogeochemical cycle, which includes conversion into methyl mercury, a toxic and bioaccumulating compound hazardous to humans, other mammals, and birds.

This same time period coincides with rapid advances in satellite remote sensing and retrieval algorithms, providing information on biomass burning on a global scale. We are now in a transition phase where remote sensing is adding to ground based reporting by providing critical data on fuel characterization, fire detection and burn area growth, fire intensity and smoke plume composition and transport.

Since this is the first inclusion of biomass burning into global mercury budgets, a description of the salient facts about the burn process and the biogeochemistry are briefly described. For more detailed insight, the reader is referred to the pertinent references in the text. We briefly discuss the following aspects:

- What is the global distribution and speciation of biomass?
- How does mercury enter the biomass?
- How is mercury distributed in biomass and organic soils?
- How does fire release mercury?
- How can we estimate emissions of mercury from fires?

8.1.1   Global Distribution of Vegetation

Figure 8.1 depicts the global vegetation mass distribution. Vegetation mass is concentrated in the tropical and subtropical zones (tropical forests and savanna and grass lands) and in the northern tiers of the globe (temperate and boreal forest). A related website (http://www.unep-wcmc.org/forest/global_map.htm) also describes all vegetation types.

8.1.2   Biogeochemistry of Mercury in Forests

Mercury in vegetation and organic soil is the result of bi-directional processes connecting atmosphere, plants, organic soils, and hydrology (Gustin et al., 2008; Lindberg, 1996; St. Louis et al., 2000; Driscoll et al, 2007). Mercury enters ecosystems mostly by wet and dry deposition of particulate Hg(p), ionic (RGM), and gaseous elementary mercury (GEM) onto live vegetation and soil surfaces, and by stomatic assimilation of GEM (Erickson et al., 2003; Frescholtz et al., 2003, Fay et al., 2007). Mercury on vegetation surfaces can be incorporated into plant tissue or photo-chemically reduced to GEM and released, or it can be washed off as throughfall. Xylem sap contribution to plant mercury is minor (Bishop et al., 1998) except for plants in soils with high mercury content, contaminated or naturally enriched. Upon deposition to the ground in throughfall or in senesced leaves,
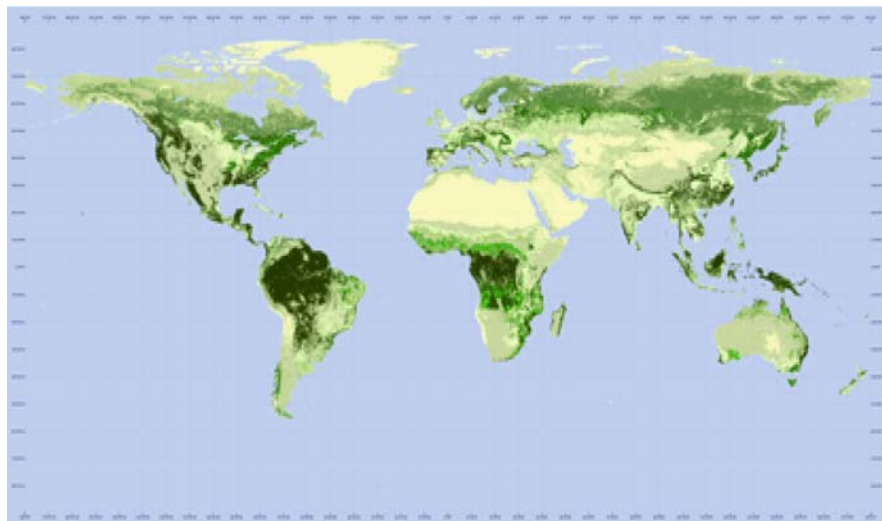
Figure 8.1 Olson's major world ecosystem complexes ranked by carbon in live vegetation: An updated database using the GLC2000 land cover product (cdiac.ornl.gov)

needles, bark and dead wood (litterfall), mercury is sequestered by reduced sulfur groups contained in the carbon pool (Skyllberg et al., 2003). This general behaviour was confirmed by the METAALICUS field experiments (Harris et al., 2007), where one mercury isotope sprayed onto live vegetation remained mostly immobilized in the organic soil, while a different isotope sprayed into water in the same region was rapidly converted into methyl mercury.

8.1.3   *Mercury Distribution in Vegetation and Organic Soil by Region*

Knowing the partitioning of mercury in the fuel pool is essential because only not all components of the fuel pool are combusted in a fire. The mercury content in plants is species- and plant-part specific. Mercury increases through the growing season with insignificant levels at leaf-out. Mature leaves and needles from deciduous, hardwood, coniferous trees in North American forests contain about 30-70 ng g^{-1} mercury determined by dry mass (dm). Similar ranges have been measured for Central- and South America, Australia and Africa. Some European oak leaves can reach 150-200 ng g^{-1} (dm). Bark contains higher mercury concentrations than leaves and the content differs between live and dead fractions. Bole wood is much lower in mercury, e.g. ~2 ng g^{-1} (dm) for aspen. Mercury in African savanna grasses ranges from 6-9 ng g^{-1} (dm), the same range as in agricultural residues (rice, corn).

Of critical importance is the partition of mercury above and below the forest surface. In temperate and boreal forests the mercury pool in the live plants amounts

to <10% of the total pool (Grigal, 2002, 2003). As an example, in a boreal forest plot in Saskatchewan, Canada, 93-95% of the mercury pool was located in the organic soil above the mineral layer (Friedli et al., 2007). The mercury concentration in the organic soil reached 300 ng g^{-1} (dm), values typical for upland boreal forests. The mercury pool in a forest depends on stand age. In the above example the mercury pool increases from ~1.0 to 2.9 to 7.8 mg m^2 for stand ages 39, 133 and 180 years, respectively. Similar data are available for temperate North American forests (Harden et al., 2004; Engle et al., 2006; Biswas et al., 2007, 2008).

Because Hg is primarily located in the organic soil layers of a forest, it is important to understand the extent of the organic soil. Carbon accumulation (i.e. photosynthesis vs. decomposition) of an ecosystem depends on climate, vegetation type and stand age, burn frequency and hydrology. Upland boreal forests and temperate forests accumulate 5-20 cm of organic soils and burn frequently, whereas lowland peat, bogs, and permafrost may accumulate carbon over 100s of years between fires and reach several meters in thickness. As a consequence these ecosystems contain much larger mercury pools, commensurate with a large carbon pool (Turetsky et al., 2006). Of particular interest are the tropical peat fields in south East Asia because of their large size and the lack of mercury data.

African and Australian savannas accumulate only 0-2.5 cm of organic soil (Shea et. al., 1996), because of frequent (annual or biannual) burning and climatic conditions that favour rapid decomposition of organic matter. Vegetation and soil mercury in the African region is poorly defined: while the carbon emissions are the largest by far for all regions, few EF(Hg) are known. Since burning is frequent, modeled deposition rates for mercury may serve as an upper limits on what level annual mercury emissions could reach. Seigneur et al. (2003) estimated wet and dry deposition in northern and southern hemisphere Africa (NHAF, SHAF) to be 8-15 μg Hg m^{-2}. Assuming that evasion, stomatic uptake and bacterial and herbivore losses are small, and fuel mass burned ranges from 1-4 kg m^{-2} yr^{-1}, EF(Hg) of 2-3.75 μg Hg kg^{-1} could be expected. This compares with 6±3 μg Hg kg^{-1} determined from mercury content in grass (Friedli et al., 2008).

Undisturbed wet tropical forests also have shallow layers of organic soil because of rapid decomposition of the vegetation by insects and bacterial activity. At a site in the Amazon, 40% of the mercury resides in live vegetation, 60% in organic soil and litter (Michelazzo et al., 2008). This is very different from boreal forests, where >90% of the mercury is contained in the organic soil. Here the mercury pool is also smaller, 0.65 mg m^{-2} compared to 1-3 mg m^{-2} in upland boreal forests.

8.1.4   Mercury Release from Burning Biomass and Organic Soil in Different Landscapes

This section starts with a general description of the mercury release process as it was investigated in controlled laboratory experiments. It then discusses the emission behaviour in wildfires burning in different landscapes and under different fire weather conditions.

The mercury release process was studied in lab-scale experiments by Obrist et al. (2007) and Friedli et al. (2001; 2003a). These studies showed that essentially all mercury is released during the flaming phase of the combustion of dry leaves, needles and small twigs; little is known about the emission from smouldering fires, which are important for organic soil combustion. The speciation of the emitted mercury is dependent on the moisture content of the fuel: dry fuels emit GEM almost exclusively; green or wet fuels generate more smoke which can include up the 40% of the released mercury in particulate form Hg(p). The available data on mercury speciation are very limited but are important because speciation influences the location of the downwind deposition of the released mercury.

Wildfires are very complex phenomena and are dependent on fuel source (composition, mass, structure, moisture content), physical setting (slope, elevation, relief, soil structure), weather (temperature, wind, humidity, insolation) and climate (e.g. drought). Depending on conditions, different heat release rates are observed. Wildfires (and prescribed fires) behave spatially and temporarily differently because of regional climatic and weather differences. After ignition by lightning, spotting or an anthropogenic source, surface fires consume surface material (grasses, mosses and lichen, litter, downed wood) and shrubs, and can transition via ladder fuel into crown fires which consume needles, leaves, small branches and bark. Mercury contained in the burned matter is essentially fully released. If the ground is ignited, the resulting ground fire (organic soil horizons, logs, wood piles, stumps) can last for days to years and release partially or fully the mercury pool, creating a mosaic of burned and unburned areas with variable amounts of residual mercury.

Boreal wildfires, particularly under drought conditions, are often severe. They have regional and global environmental impacts because they frequently inject combustion products, including mercury, into the stratosphere (Fromm and Servranckx, 2003). The plumes undergo long-range transport and chemical transformations: mercury reactions include the conversion of GEM into Hg(p) and RGM, which have shorter lifetimes. Boreal fire plumes transported over long distances have been observed for North America (e.g. Sigler et al., 2003) and Western Russia (Witham and Manning, 2007). Intense boreal fires can generate pyro-cumulus clouds and intensive local precipitation, which could result in mercury deposition and hotspots on the ground.

Fires in dry tropical and extra-tropical temperate forests exhibit fire dynamics commensurate with fuel density, vegetation speciation, surface geography, and weather and climatic conditions.

In tropical savanna fires the heat release is smaller and stratospheric injection is less likely. The fuel mass available for burning in these ecosystems varies substantially depending on past rainfall or drought, e.g. on El Niño cycles for African savannas.

Undisturbed wet tropical forests have a 100 to 1000 year fire frequency. Where deposition mercury ends up in these ecosystems is unclear: there is little organic soil to sequester mercury as would happen in northern forests. Does it evade from the litterfall back into the atmosphere, is it absorbed into the mineral layer, or is it hydrologically removed? Commercial deforestation in tropical forests resulting in complete burning of all fuel mass removes all mercury, including from bole wood and stumps.

8.1.5   Estimation of Mercury Emissions from Biomass Burning

Mercury emission estimates from biomass burning are based on carbon budgets in combination with emission factors for mercury, EF (Hg), related to carbon released. To achieve a uniform, globally consistent treatment of carbon release for all observed fires, we selected a sophisticated carbon emission model, the Carnegie-Ames-Stanford-Approach (CASA) biogeochemical model, specifically modified to account for biomass burning (hereinafter termed as the Global Fire Emission Database version 2 (GFEDv2) as described by van der Werf et al., 2006), which partitions observed global fires into regions with similar fuel types and fire behaviour. Emission factors for mercury for different ecosystem types originate from two methods: (1) ground-based measurements of the difference in mercury pools before and after a fire, and (2) enhancement ratios (ER) of Hg and CO in plumes measured on the ground or by aircraft. Mercury emissions are then estimated as the product of carbon emissions and mercury emission factors.

8.1.6   Carbon Emission Model

The release of carbon from large-scale biomass burning is traditionally estimated from the amount of biomass (or fuel) burnt, which is calculated as a product of 1) the areal extent of the burn (burned area, BA), 2) the amount of fuel available for burning (fuel load, FL), and 3) the fraction of fuel load that has been combusted (combustion completeness, CC), integrated across space and time of interest (Seiler and Crutzen, 1980). Due to the inherent complexity of wildfires, and biomass burning in general, the estimates of these three components exhibit large spatial and temporal variability that limits our assessment of the accuracy of carbon emissions. Early studies estimated the carbon release by developing inventories (e.g. from fire management agencies) for each of these components and for different biome types, and extrapolate these inventories using global vegetation maps to continental or global-scale estimates (e.g. Hao and Liu, 1994). However, over the past two decades, these methods are being supplanted, primarily due to the increased availability of biogeochemical and fire-related observations from space (remotely-sensed), in conjunction with ground-based studies on fuel loads (and consumption), airborne measurements of smoke plumes, as well as the advancements in biogeochemical and transport models. We briefly describe below the current methods of estimating each of these components, with a particular focus on integrated approaches in estimating the carbon release on a regional to global spatio-temporal scale (e.g. GFEDv2, van der Werf et al. 2006). This type of approach provides a consistent and traceable representation of global carbon emissions, which can be very useful in evaluating and interpreting estimates with ground truth and other independent datasets. Please refer to van der Werf et al. (2006) for more details on the carbon emission model used in this report.

Burned Area

Global burned areas can be derived from detection of active fires from multi-sensor satellite imageries (ATSR, AVHRR, MODIS, VIRS) and the relationship of fire counts to burned area (e.g. Giglio et al. 2006). Estimates of burned area are now available for specific regions, typically from forest services and fire management agencies (e.g. Canada Forest Service) and from country reports (e.g. Forest Resource Assessment, or FRA). These regional estimates serve as basis for validating burned area estimates developed at a global scale. Most recently, burned area products derived from satellite observations of burn scars became available for the year 2000 at a monthly time scale and 1km x 1km spatial resolution. Of these products, the GBA 2000 (Gregoire et al., 2002) is based on the SPOT-VEGETATION instrument, while GLOBSCAR (Simon et al., 2004) is generated from data collected by the ATSR instrument. Detailed comparisons between these two products against country reports reveal key differences. Most notably, GBA 2000 has substantially higher burned area results in Africa and Australia, which Simon et al. (2004) attributed to inability of GLOBSCAR algorithms to detect large areas of burning in woodlands and shrub lands. Other than these two regions, the two products appear to be generally similar at continental scales (Kasischke and Penner, 2004).

   From the evaluation of Giglio et al. (2006), the burned area reported in GFEDv2 appears to be in general agreement with Canadian Interagency Forest Fire Centre (CIFFC) compilations (slope about 70%) and US National Interagency Fire Center (NIFC) statistics (slope about 83%) with some degree of underestimation for very large burned areas. For Russia, the burned area estimate in 2001 is about 26% larger than reported by Sukhinin et al. (2004). Globally, the estimates are larger than GBA 2000 (by about 32%) and GLOBSCAR (by about 144%). The average annual burned area in GFEDv2 for the years 1997-2006 is about 332 ± 26 Mha yr^{-1}. The majority is due to burning in Africa (66%), followed Australia (13%), Asia (10%) and South America (5%).

   On average, uncertainties in GFEDv2 global burned area estimates appear to be smaller (20-30%) than earlier estimates which had uncertainties over a factor of 2 (Kasischke and Penner, 2004). However, the differences in GFEDv2 burned area with other estimates can be large during some years and on local to regional scales. One of the shortcomings of these satellite-based estimates is their difficulty to detect small burned areas, particularly in deforestation regions with persistent cloud cover and mechanized clumping of fuels. In addition, the ability to globally validate these satellite-based estimates remains problematic due to the lack of validation data from ground-based measurements.

Fuel Loads

The available fuel load is defined here as organic matter available for combustion and includes all above-ground herbaceous biomass, above-ground woody biomass, coarse woody debris, and litter. Regional information on fuel loads are either

derived from inventory-based compilations of fuel load maps (e.g. ECE-FAO, IFFN reports) or from satellite observations of vegetation indices (e.g. Barbosa et al., 1999). More recently, estimates on available fuel loads employ biogeochemical models that simulate the carbon fluxes across the different pools of the terrestrial biosphere (e.g. foliage, woody materials such as branches, stems, boles and roots, litter, active and passive soil), including carbon losses from fires, herbivores, and fuel wood collection. In most cases, these biogeochemical models employ added constraints from satellite-derived estimates of net primary production (e.g. from NDVI, normalized differential vegetation index) and leaf-area index (LAI), together with maps of soil moisture, temperature, precipitation, soil types, and vegetation types to realistically represent the spatio-temporal patterns and amount of biomass across different ecosystems. This approach integrates process-level information of large-scale vegetation dynamics with important drivers of fuel loads that will likely respond to global change processes. In GFEDv2, the biogeochemical model employed is the Carnegie-Ames-Stanford-Approach, CASA, (Potter et al. 1993) with a spatial resolution of $1^{o}x1^{o}$ and a temporal resolution of one month. The model uses the combination of satellite-derived estimates of fraction of incident photo synthetically active radiation (PAR) absorbed by the green plant canopy (fAPAR) from SeaWIFS (Behrenfield et al. 2001) and satellite-based estimates of solar insolation for PAR (Bishop and Rossow, 1991) to simulate net primary production (NPP). Please refer to van der Werf et al. (2006) for specific details on the allocation of NPP to different carbon pools. In GFEDv2, CASA was specifically modified to account for fire by the addition of satellite-based estimates of burned area (Giglio et al. 2006) to adjust for the potential loss of above-ground biomass and litter due to fire. In cases of fire, a direct loss of carbon is initiated from above-ground carbon pools depending on fire mortality and combustion completeness (van der Werf et al. 2006).

Other recent global studies using the biogeochemical approach, include Hoelzemann et al. (2004) who used the Lund-Postdam-Jena (LPJ) Dynamic Global Vegetation Model (DGVM), and Jain et al. (2006) who used the terrestrial component of the Integrated Science Assessment Model (ISAM). Regional-scale emission models have also been employed to refine estimates for specific regions of the globe that are highly susceptible to fires (e.g. Kasischke et al., 2005 for the boreal region, Hély et al., 2003 for Africa, Wiedinmyer et al., 2006 for North America).

The average fuel load (in kg dry matter m^{-2}), calculated from GFEDv2 for the year 2000 across regions of similar vegetation types, ranges from 1.3 ± 1 kg m^{-2} in non-forests, 18 ± 21 kg m^{-2} in tropical forests (mostly equatorial Asia), to 10 ± 8 kg m^{-2} in extra tropical forests (including boreal). These estimates are comparable on aver-age to field measurements (Guild et al., 1998; Hobbs et al., 1996; Kasischke and Bruhwiler, 2002; Shea et al., 1996) and appear to have uncertainties on a regional scale, of about a factor of 2. A large part of the uncertainty is attributed to poor representation of soil organic carbon and below-ground biomass, especially in boreal regions and peat lands. In GFEDv2, highest fuel loads are predicted over equatorial Asia and boreal regions, where soil organic carbon represented a large fraction of the fuel load. The fuel loads in boreal North America and boreal Asia were approximately 8 kg m^{-2}, while in savanna regions, the fuel loads were highest in southern hemisphere Africa

(3 kg m^{-2}) where significant burning occurred in woodland areas and lowest in Australia (0.8 kg m^{-2}), where much of the burning occurred in grasslands.

Combustion Completeness

Combustion completeness (CC) is defined here as the ratio of fuel consumed from fires to total available fuels. Measurements of combustion completeness vary across a wide range of vegetation types (Shea et al., 1996; Hoffa et al., 1999, Carvalho et al., 2001). In general, they are associated with the types of fuel, fuel loads, and fuel configurations (including water content) but may also vary significantly depending on fire practices, fire severity and dynamics. The values range from 1 (complete combustion) for well-aired and dry litter (fine fuels) to about 0.2 for coarser fuels like stems and woody debris, which burn incompletely. Foliage and twigs in boreal regions, for example, have high CC while its living stems and boles have low CC. Studies have also shown that CC varies during the burning season, with a tendency to increase when fuels have more time to dry out (Shea et al. 1996).

In GFEDv2, CC is allowed to vary in the biogeochemical model across the different carbon pools and from month to month. CC values range from 0.8-1.0 for leaves, 0.2-0.3 for stems, 0.9-1.0 for fine leaf litter, 0.5-0.6 for coarse woody debris and 0.9-1.0 for soil organic carbon. In addition, CC is increased in stems and coarse litter in areas with high levels of fire persistence.

Uncertainties in CC can be attributed (yet difficult to quantify) to the lack of direct observations on fire behaviour across different ecosystems and throughout the burning season. Also, differences in fire practices across difference regions may increase the uncertainty. For example, in tropical forests undergoing deforestation where mechanized clumping is prevalent, it is observed that CC tends to approach to 1.0 over the course of the burning season as fuels are piled and ignited multiple times (van der Werf et al., 2006).

Fuel Consumption

The amount of biomass burned (fuel consumed) is a product of burned area, fuel load and combustion completeness. The release of carbon from biomass burning is then calculated by assuming a carbon content of 45% of the dry biomass (Andreae and Merlet, 2001). Thus, estimating the uncertainty in fuel consumption has a tendency to be multiplicative.

8.1.7 Mercury Emission Factors

Emission factor, EF(Hg), estimation for this work is based on two different methodologies: one is centered on plume composition, measured at ground level or by aircraft; the second is based on the change in the mercury pool in soils before and

after a fire. Soil-based mercury is reported as g Hg released per area burned (ha or m^2); plume-based EF(Hg) have the units μg Hg per kg fuel burned. The conversion between EFs requires fire-specific values for fuel burned per unit area, which in most cases are estimates.

Mercury in plumes is measured in ng Hg/ (std) m^3 and the corresponding carbon equivalent in the same volume is calculated from measured CO_2 + CO (or estimated as 9:1 (molar) from CO measurements), corrected by a factor of 1.05 to account for carbon in trace components CH_4, particulates, non-methane organic compounds (NMOC). For the conversion of carbon to dry mass fuel, an average factor of 0.45 for carbon in fuel is assumed (consistently with the carbon model described above). All emitted mercury species (pHg, GEM, and RGM) must be included in the analysis. Mercury emission factors determined from plume observations are generally under-estimates because some pHg is lost by deposition before it can be sampled. In nascent plumes, pHg is a significant fraction of the mercury emitted, up to 40% (Friedli et al., 2003a, Friedli et al., 2003b, Obrist et al., 2007). Measurements made far from a fire event may additionally miss the mercury lost by conversion to and deposition as pHg along the plume track. For these two reasons, most plume studies are underestimates.

A convenient method to assess mercury in fire plumes is to measure the enhance-ment ratio (ER) which is defined as Δ[Hg]/Δ[CO], Δ where Δ[Hg] is the sum of all species in excess of background concentration and Δ[CO] is the difference between CO concentration in the plume and the background. For this work we have assumed that the ratio between EF (μg/kg fuel) and ER (molar) is constant for all fires and related by a factor of 1425, derived from the most robust aircraft data available (Friedli et al. 2003b: 113 ± 59 μg/kg fuel burned and its corresponding ER of 0.793 × 10^{-7} (Δ [Hg]/Δ[CO]). To convert ER into emission estimates, a corresponding CO source term is required. Table 8.1 lists ER from ground and aircraft-based measurements for different regions.

The average of all measurements in Table 8.1 is 1.54 × 10^{-7} (mol/mol) corresponding to EF(Hg) of 220 μg Hg/kg fuel based on Friedli et al. (2003b), from which both ER (Δ[Hg]/Δ[CO] and EF(Hg) are available.

The advantage of the plume method is its integrative nature, averaging variation in fire dynamics and fuel composition, and giving a relatively broad spatial coverage. The disadvantage is the requirement for an instrumented aircraft on standby.

Table 8.1 Published molar enhancement ratios (ER) observed from fire plumes worldwide

Location	ER (Δ[Hg]/Δ[CO])	Reference
Washington State (ac)	(0.79 ± 0.04) × 10^{-7}	Friedli et al. (2003b)
Pacific NW (ground)	(1.46 ± 0.9) × 10^{-7}	Weiss-Penzias et al. (2007)
Alaska (ground)	(1.57 ± 0.67) × 10^{-7}	Weiss-Penzias et al. (2007)
Quebec (ac)	2.04 × 10^{-7}	Friedli et al. (2003a)
Quebec (ground)	0.86 × 10^{-7}	Sigler et al. (2003)
South Africa (ground)	(2.1 ± 0.21) × 10^{-7}	Brunke et al. (2001)
South America (ac)	(1.17 ± 0.15) × 10^{-7}	Ebinghaus et al. (2007)
South America (ac)	(2.39 ± 0.99) × 10^{-7}	Ebinghaus et al. (2007)

where ac = aircraft measurements and ground = ground measurements

The soil-based method applies to biomes where mercury resides predominantly in the organic soil, i.e. boreal and temperate forests. It is based on the difference in the mercury pools in organic soil in adjacent plots before and after a fire

Table 8.2 Emission factors (EF in $\mu g/kg$ fuel) used in the emission calculations

Reference	Method	EF Range	EF Mean	Notes[2]	Fuel Burned[3]
Boreal Forest					
Harden et al. (2004)	S	0 - 138	69	Alaska, Conif. Forest, (PB)	2.5
Friedli et al. (2003a)	P	112 - 112	112	Quebec, Pine Forest, (W)	2.5
Sigler et al. (2003)	P	60 - 60	60	Quebec, Pine Forest, (W)	2.4
Cinnirella & Pirrone (2006)	P	62 - 112	87	Siberia, (W)	5.6
Weiss-Penzias et al. (2007)	P	136 - 278	207	Alaska, (W)	2.5
Turetsky et al. (2006)	S	90 - 297	193	Alaska, Upland, (W)	2.5
Turetsky et al. (2006)	S	535 - 2417	1476	Alaska, Lowland, (W)	2.9
Mean		142 - 488	315		
Temperate Forest					
Friedli et al. (2003b)	P	54 - 172	113	Washington, Mixed Forest, (W)	2.5
Brunke et al. (2001)	P	78.7 - 163.4	121	South Africa, Fynbos, (W)	2.5
Engle et al. (2006)	S	80 - 204	142	California, Conif. Forest, (PB)	2.5
Engle et al. (2006)	S	88 - 196	142	Nevada, Coniferous Forest, (W)	2.5
Biswas et al. (2006, 2008)	S	168 - 348	256	Washington, Mixed Forest, (R)	2.5
Biswas et al. (2007)	S	296 - 1012	654	Wyoming, Coniferous Forest, (W)	2.5
Biswas et al. (2007)	S	144 - 516	402	Wyoming, Aspen Forest, (W)	2.5
Woodruff et al. (2001)	S	80 - 80	80	Minnesota, (PB)	2.5
Mean		124 - 336	239		
Sage-Chaparral (Shrublands)					
Engle et al. (2006)	S	18.7 - 39.9	29.3	Nevada, Sage, W	1.84
Cinnirella & Pirrone (2006)	P	52.8 - 52.8	52.8	Mediterranean, W	1.25
Mean		35.8 - 46.4	41.1		
Grasslands and Ag. Waste					
Obrist et al. (2007)	L	7.8-9.8	8.8	Rice straw	
Friedli et al. (2008)	L	3-9	6	South African savanna	
Friedli et al. (2003)	S	38	38	Oregon, Wheat	3.06
Mean		3-38	18		

[1]Type of method used, soil (S), plume (P), or laboratory (L)
[2]Type of fire, wildfire (W), prescribed burn (PB), Rex fire (R)
[3]in kg fuel m^{-2} burned; used for EF(Hg) calculation. When nothing else was available, 2.5 *kg* fuel m^{-2} burned was assumed (based on Amiro et al. 2001). All others are from respective references.

(Harden et al., 2004; Biswas et al., 2007, 2008; Engle et al., 2006; Turetsky et al., 2006). In temperate or boreal forests, mercury resides >90% in the organic soil. Since the above ground mercury fraction is only <10% of the total Hg pool, it was neglected in the references given for boreal or temperate northern forests. Release of Hg from the underlying mineral layer is also negligible (Engle et al., 2006). The advantage of the soil-based method is that it requires only total mercury measurements in the organic soil. The disadvantage is poor statistics because of large short- and long-range spatial variability and inconsistent response to fire dynamics.

One direct comparison of the two EF(Hg) estimation techniques has been accomplished. Measurements in the fire plume from the Rex fire in Washington State were made from an aircraft during the burn (Friedli et al., 2003b) and soil measurements were made post-fire in adjacent burned and unburned sites (Biswas et al., 2006, 2008). As expected, the soil-based release estimate was higher, 6.4 ± 1.1 g Hg ha^{-1} as compared to 2.9 ± 2.2 g Hg ha^{-1} from the aircraft measurements. The available references for both methods are combined in Table 8.2 and arranged by ranges and means for different landscapes. The means are unweighted averages of all measurements in each vegetation type. The uncertainties in the reported values results from many contributions, including the influence of burn severity, inclusion of measurements of all mercury species, paucity of measurement for all fuel types (especially for grasses, shrubs and agricultural waste products) and uncertainties in the emission factor estimation technique.

The amount of fuel burned during a fire is highly variable among different ecosystems, and even within the same vegetation types (Amiro et al., 2001, French et al., 2004). Yet, a value for fuel burned is needed to determine emission factors. The means from Table 8.2 were applied to the three land classifications used in the carbon emission model, i.e. to tropical forests, extra tropical forests and non-forested land, and applied as indicated in Table 8.3 to the regions selected for the carbon emission model.

8.2   Results and Discussion

8.2.1   *Global Distribution of Carbon Emissions*

The average monthly spatial distribution of carbon emissions from GFEDv2 are shown in Figure 8.2 These represent the model-predicted mean seasonality of carbon released from large-scale biomass burning during the most recent decade (1997-2006). As has been noted in previous studies, the biomass burning activity across the globe varies, depending on vegetation types and climate conditions, as well as fire cultural patterns, which correlate well with agricultural practices and land use, particularly in Africa, South America and Asia (e.g. Duncan et al., 2003). Globally, biomass burning occurs at all times of the year, with a distinct peak in July-September and a lower peak in December-February. A large fraction of this peak is due to fires in Africa during the dry season. In Northern Hemisphere Africa, burning occurs in winter dry season within the savanna ecosystems (e.g. Sahara desert and central

Table 8.3 Emission factors used in this report (in *μg* Hg/*kg* fuel)

Region	Extratropical	Non-Forest	Tropical
BONA	315	41	
TENA	242	41	
CEAM	242	41	198
NHSA	242	41	198
SHSA	242	41	198
EURO	242		
MIDE	41		
NHAF	242	41	198
SHAF	242	41	198
BOAS	315	41	
CEAS	242	41	198
SEAS	242	41	
EQAS		41	315
AUST	242	41	198

Please refer to Figure 8.4 for definition of regions.
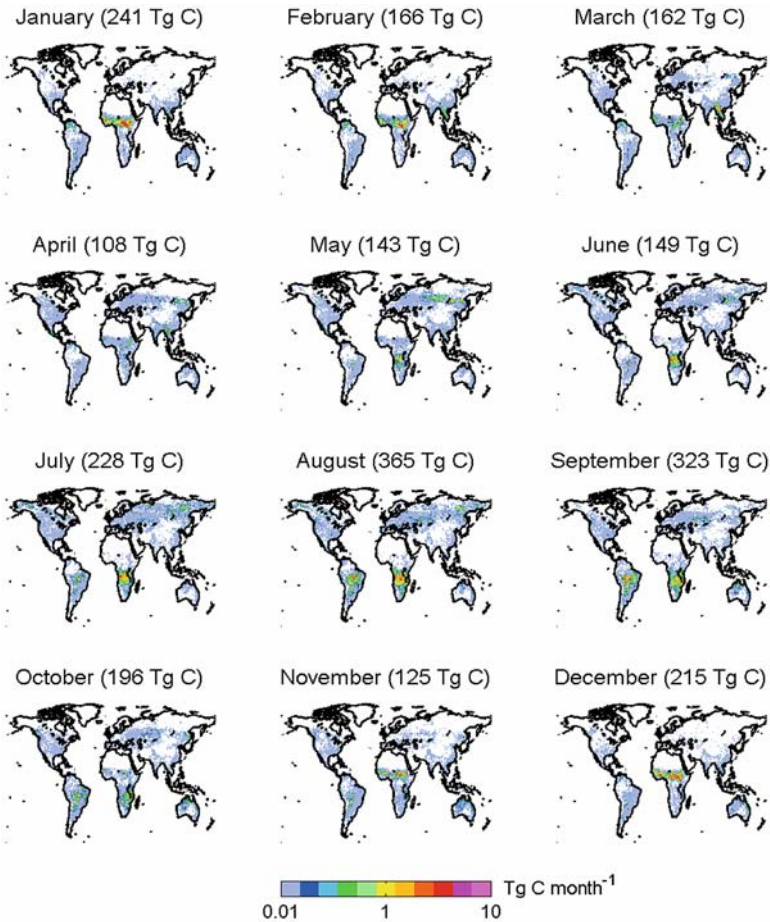
Figure 8.2 Average monthly carbon emissions for the period 1997-2006

African rain forests). It begins in the Sahel in October and spreads south through November with highest burning activity in December and January.

On the other hand, fires in the Southern Hemisphere Africa typically start in the woodlands of Zaire and Congo by early June and continue to peak across the southeast in the grasslands and shrub lands of Angola, Zambia and Tanzania during August through September and Mozambique in October. A similar fire pattern occurs in South America, mostly in the cerrados of Brazil and along the arc of fire (or deforestation) in the Amazon rainforest, generally in August through September.

Fires in tropical Asia (Indonesia, Malaysia and the rest of Southeast Asia) are highly variable and are usually associated with very dry conditions, like El Niño events, enabling land-owners to use fire more efficiently as a tool for land-clearing in the region. Because of the large peat deposits in Indonesia that are exposed during land-clearing, the carbon emissions in equatorial Asia is significantly high during El Niño years (e.g. 1997-1998). Burning typically occurs in March-April over Southeast Asia and in August-October in equatorial Asia.

Fires in Central America peak during April to June mainly due to deforestation and agriculture, while much of the bush fires in Australia occur in the shrub lands in northern Australia and to some degree in southeast Australia during September through December.

In the Northern Hemisphere temperate and boreal regions, a large fraction of fires are caused by lightning. Boreal forest fires generally take place in May to September when temperatures and lightning frequencies are high. Fires in boreal Asia typically start in May around Mongolia and spread north in Siberia during summer. Like equatorial Asia, fires in the boreal regions are also affected by droughts and very dry conditions. For example, fires in Alaska, Canada and Siberia were especially high in 1997-1998 and 2004 (e.g. Kasischke and Bruhwiler, 2002). Consequently, releases of carbon are significantly high during these years also due to characteristically higher fuel loads (e.g. soil organic carbon) in these regions. Burning in western Russia and Europe is mostly associated with agriculture and generally occurs during spring through fall, while burning in the continental U.S. is associated primarily with forest wild fires and prescribed burning generally occurring from June to September. Carbon release from biomass burning in the continental U.S. is small relative to emissions from boreal forests in Alaska and Canada.

8.2.2   Global Distribution of Mercury Emissions

We present in Figure 8.3 and Table 8.4 the associated mercury emissions as calculated in this work using carbon emissions as basis for biomass burning activity (Section 2.6) and applying emission factors that we have compiled for the globe (Section 2.7). Similar to Figure 8.2, the distribution represents the mean seasonality for the period 1997-2006.

Overall, we find a strong correlation of mercury emissions with carbon emissions from biomass burning shown in Figure 8.2, which as can be expected, highlights
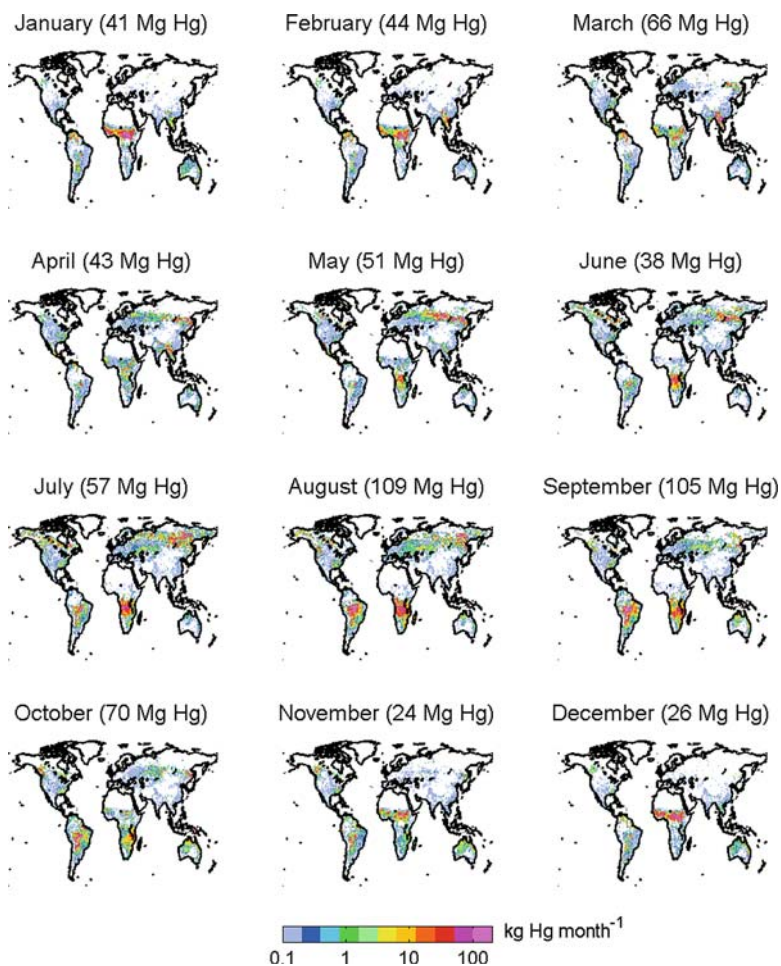
Figure 8.3 Average monthly mercury emissions for the period 1997-2006

Table 8.4 Mean seasonality of global mercury and carbon emissions (1997-2006)

	Hg *(Mg)*	Carbon *(Tg)*	Burned Area *(Mha)*	Effective EF(*μg Hg / kg fuel*)
Jan	41	241	46	77
Feb	44	166	23	120
Mar	66	162	15	184
Apr	43	108	11	177
May	51	143	15	160
Jun	38	149	16	116
Jul	57	228	24	112
Aug	109	365	34	134
Sep	105	323	35	147
Oct	70	196	26	161
Nov	24	125	31	86
Dec	26	215	55	56

the general influence of the spatio-temporal variability of global fire patterns to the release in mercury from vegetation. In this work, the emission of mercury is a function of burned area, fuel load, combustion completeness and emission factor, each of which has its associated uncertainties.

A key finding of this exercise is the significant impact of fires in the boreal region and in the tropical forests of Asia and South America, to the distribution of mercury emissions across the globe. While we find that the majority of carbon emissions can be attributed to fires in African savannas, our results for mercury emissions show major contributions from equatorial Asia, boreal Asia and Southern Hemisphere South America. The model also predicts a slightly different seasonal peak in mercury emissions, which are strongest in August and March compared to carbon emissions that are strongest in August and December. This is mainly due to the strong influence of high emission factors for these forested regions and low emission factors for fires in the savannas. In general, the fuel load and combustion completeness (CC) are inversely related, with lower CC in areas with high fuel loads (Section 2.5); hence having a compensating effect to emission estimates. As a consequence, this effect highlights the sensitivity of the emissions to estimates of burned area and assumed emission factors. Furthermore, this result indicates that while uncertainties on estimates of carbon emissions from fires in savanna (as well as burning from agricultural waste) play an important role, they are less significant with regards to mercury.

In addition, we note that the major sources of mercury from fires occur in regions where transport plays an important role in the distribution of atmospheric mercury across the globe. In particular, mercury released from fires in equatorial Asia and tropical South America can be transported to higher altitudes due to strong convection in these regions and can then be dispersed efficiently over a larger area. In a similar manner, mercury released in boreal regions can be injected at relatively higher altitudes, thereby largely influencing the distribution of mercury in the Northern Hemisphere middle to high latitudes.

8.2.3 *Regional Estimates of Carbon and Mercury Emissions*

We report in this section our estimates of carbon and mercury emissions from biomass burning for different regions. Here, we used the regional divisions from the carbon emission model (please refer to Figure 8.4) in generating a regional budget for annual sources of carbon and mercury as shown in Figure 8.5 with corresponding values in Table 8.5. This annual budget is an average for 1997-2006.

We estimate a global source of mercury from biomass burning of about 675 ± 240 Mg yr^{-1}. As noted earlier, there is a distinct shift in regional contributions of mercury emissions to the global budget relative to regional contributions of carbon emissions. On a process level, we find a clear correlation of burned area with carbon emissions (r=0.55) but not with mercury emissions, again indicating the dependency of mercury emissions on variability in EF(Hg)'s.

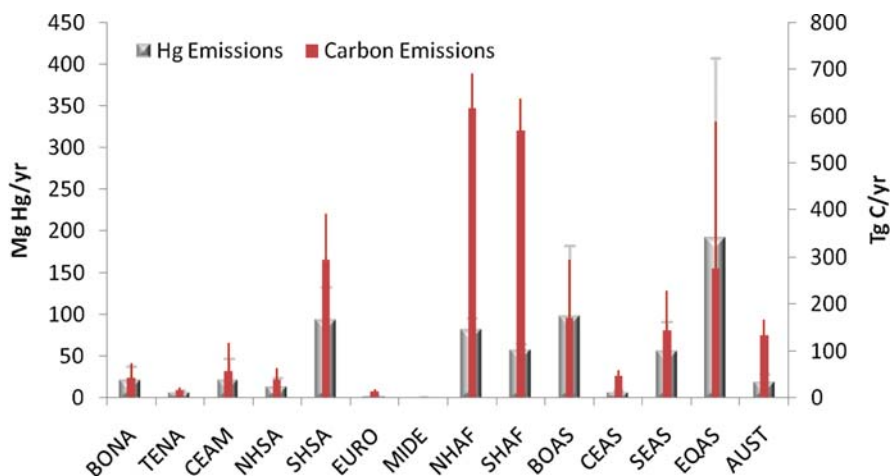**Figure 8.4** Map of regions used in GFEDv2 (from van der Werf et al. 2006)

Figure 8.5 Average annual emissions of mercury and carbon (for 1997-2006)

The major sources of mercury come from equatorial Asia or EQAS (28%), boreal Asia or BOAS (15%) and southern hemisphere South America or SHSA (14%), and only in part from northern hemisphere Africa or NHAF (12%), southern hemisphere Africa or SHAF (9%), southeast Asia or SEAS (8%), central America or CEAM (4%) and Australia or AUST (3%). Temperate North America or TENA (1%), boreal North America or BONA (3%), and central Asia or CEAS, northern hemisphere South America or NHSA, Europe or EURO and Middle East (MIDE) combined (2%) contribute little to the global budget.

This result has important policy implications with regards to assessing and regulating the impact of mercury to ecosystems and human health. We note however

**Table 8.5** Regional emission estimates for mercury and carbon (1997-2006)

Regions	Hg (Mg yr⁻¹) Mean	SD	Carbon (Tg yr⁻¹) Mean	SD	Burned Area (Mha yr⁻¹) Mean	SD	Effective EF (µg Hg/kg fuel) Mean
BONA	22	16	42	30	2	1	233
TENA	6	3	16	6	2	0	178
CEAM	22	25	56	61	3	2	175
NHSA	13	10	38	25	4	1	157
SHSA	95	39	294	97	12	2	145
EURO	2	1	14	5	2	1	72
MIDE	0	0	1	0	0	0	17
NHAF	83	13	618	74	141	13	60
SHAF	58	7	571	68	78	9	46
BOAS	99	83	170	124	9	5	263
CEAS	7	2	47	12	17	5	67
SEAS	57	35	144	84	12	5	177
EQAS	192	216	276	312	4	4	312
AUST	19	9	133	35	46	18	65
Global	675	240	2420	382	332	26	279
Boreal (BONA+BOAS)	121	85	212	128	11	5	248
Temperate (TENA+EURO+MIDE)	9	3	30	7	4	1	89
Rest of the World	545	224	2178	360	316	26	134

\# SD for standard deviation

that there is a significant variability (as shown from the error bars) throughout the 10-year period, particularly for EQAS. We further discuss the inter-annual variability and comparisons with other regional estimates in the succeeding sections.

8.2.4 Inter-annual Variability of Mercury Emissions

Shown in Figure 8.6 are annual emissions for different regions during the 10-year period chosen in this report. As can be seen, there is a large inter-annual variability of mercury emissions across different regions, particularly in EQAS, SHSA, BOAS, BONA and CEAM. There were large amounts of mercury released during the strong El Niño year of 1997-1998 and during drought conditions in 2003-2004. The bulk of this inter-annual variability occurred in Indonesia where peat deposits were available as fuel loads, as well as in boreal region and in deforestation regions of tropical America. On the other hand, there is a more or less uniform contribution of mercury emissions to the global budget from Africa for the 10-year period. The difference in inter-annual variability is also reflected in the mean estimates discussed in the previous section and is consistent with previous studies on biomass burning (e.g. Duncan et al., 2003; van der Werf et al., 2006). Indeed, there is a clear indication of a strong relationship between biomass burning, precipitation and temperature in conjunction with fire practices in different regions.
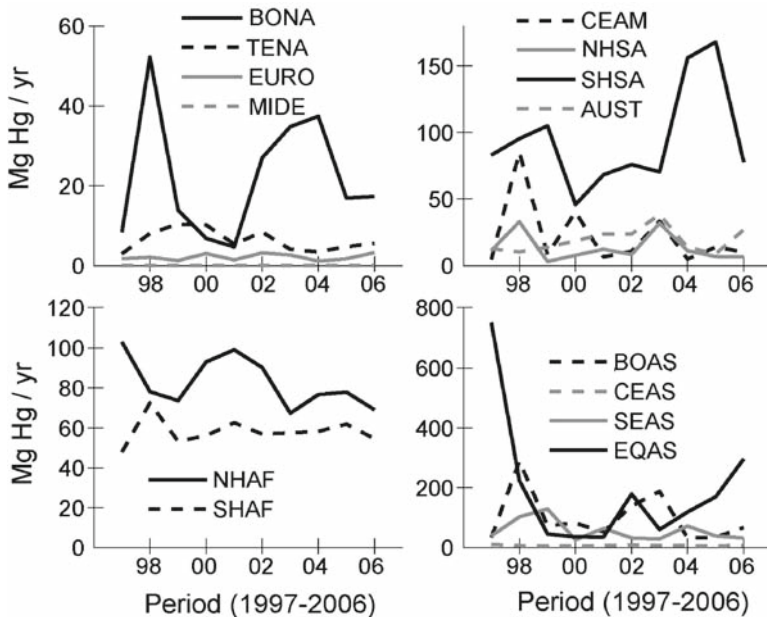
Figure 8.6 Annual mercury emissions for 1997-2006 (see map for region description)

On a regional scale, the interannual variability is significantly larger. This impact can be seen for example from fires in boreal North America, where large amounts of mercury were released during the extreme fire seasons of 1997-1998 and 2003-2004, relative to non-major fire years such as during 2000 (Turetsky et al., 2006). This is consistent with observations of other trace gases like CO, where it was observed that fires in Alaska contributed to poorer air quality in continental U.S (e.g. Pfister et al., 2004).

8.2.5 *Global Hg Emissions using Global CO Emission Estimates*

An alternative approach to estimating mercury emissions from biomass burning is to use data-constrained biomass burning inventories for trace gases. CO is highly correlated with mercury in smoke plumes from biomass burning (e.g. Friedli et al., 2003b). Inventories of CO from biomass burning have been compiled based on carbon emission models and observed emission factors (bottom-up approach). More recently, the availability of CO ground-based, airborne, and remotely-sensed measurements provided stronger constraints for CO sources (top-down approach), particularly CO from biomass burning which exhibits a large spatio-temporal variability.

Using a global average emission factor for mercury, as described in section 2.7, we show in Table 8.6 our global estimates of mercury emissions based on various

Table 8.6 Global Hg emissions based on global CO emission estimates

	CO[a]$(Tg\ yr^{-1})$	Hg[b]$(Mg\ yr^{-1})$
Bottom-up Approach		
Andreae and Merlet, 2001	465	1023
Brunke et al. 2001	612	1346
Duncan et al. 2003	437	961
Ito and Penner, 2004	264-421	581-926
Hoelzemann et al. 2004	202-571	444-1256
Jain et al. 2006	438-568	964-1250
van der Werf et al. 2006	433	953
Top-down Approach		
Bergamaschi et al. 2000	722	1588
Petron et al. 2004[c]	322	708
Arellano et al. 2006[c]	501-563	1002-1239
Muller and Stavrakou, 2005[c]	359	790

[a]climatological estimate
[b]using an average EF of 220 μg Hg/kg fuel (see Table 8.1)
[c]uses CO coentration (or burned area) data for the year 2000

CO inventories. We note here that some of the inventories are based on carbon emission models, but are constrained and updated by other independent datasets to better match atmospheric CO concentrations. Even so, these inventories have associated uncertainties, such as representation of CO transport in global chemical transport models, which need to be accounted for. Estimates for global mercury emissions range from (708 to 1346 Mg Hg yr^{-1}), which are higher than the 675±240 Mg yr^{-1} estimates derived from the GFEDv2 model and the selected EF(Hg), confirming uncertainty and variability in the emissions. While this approach considers a global emission factor for mercury along with a global CO emission estimate (and oversimplifies the spatio-temporal heterogeneity), this serves as independent general assessment of global mercury emission estimates and its uncertainties.

8.2.6 *Comparison with Other Regional Emission Estimates*

The essence of this work is the application of a globally consistent model to build up fuel pools and to estimate the carbon release resulting from combustion, to follow the process by remote sensing techniques and combine the carbon emissions with mercury emission factors, EF(Hg), to estimate global mercury emissions. Our model approach has limitation in fire detection and carbon emission uncertainties and does not always reflect regional fire practices, e.g. differences between wildfire and slash and burn fires. At this stage of sophistication, it would be unreasonable to expect full agreement with regionally collected estimates. However, global estimates appear to be reasonable as indicated by the fact that carbon and CO based approaches give similar results. In the following paragraph we compare results from the GFEDv2 model and literature values for the same regions. Shown on Table 8.7 are the key parameters used in our estimates and those from the literature.

Table 8.7 Comparison of estimates of carbon (C) and mercury (Hg) emissions with literature

Regions	Hg (Mg yr^{-1})	C (Tg yr^{-1})	Burned Area (Mha yr^{-1})	Fuel Burned (kg m-2) dm (normal)	Effective EF µg Hg kg^{-1} dm (normal)
Mediterranean[1]					
This work	2.30	9.9	1.87	1.2	104
Cinnirella et al. (2008)	4.3	17.3	0.3	12.4	112
Russia[2]					
This work	100 ± 83	177 ± 124	11 ± 4.9	3.54	254
Conard & Davidenko (1996)	(63)	82.1	7.3	2.5	345
Lavoué et al. (2000)	13.4-31.0	40.5	3.6	2.5	124-345
Cinnirella & Pirrone (2006)[*]	13.3 ± 10.5	52.92	2.1 ± 1.7	5.6	112
Cinnirella & Pirrone (2006)[#]	16.1 ± 7.3	115.83	3.9 ± 1.8	6.6	112
China[3]					
This work	2.22 ± 0.58	7.8 ± 1.5	1.9 ± 0.5	0.93	127
Streets et al. (2005)	10.9	82.1			60
USA[4]					
This work	7.2 ± 2.2	26 ± 11	2.33 ± 0.7	2.5	123
Wiedinmyer & Friedli (2007)	20.3 (43)	40.1	3.7	2.4	228
Amazon[5]					
This work	108			5.4	145-157
Michelazzo et al. (2008)	8.7-90			10.6	50/61

[1]for year 2006, with regions as described by Cinnirella et al. (2008)
[2]average for 1997-2006, with regions as described by Cinnirella and Pirrone, (2006)
[3]average across 1997-2006, with regions as described by Streets et al. (2003)
[4]average across 2002-2006, with regions as described by Wiedinmyer and Friedli (2007)
[5]average across 1997-2006, with SHSA region as defined in Figure 8.4
[#]from ground-based data for 1996-2001
[*]from remote-sensing data for 1996-2002

Mediterranean: The estimate from Cinnirella et al. (2008) for mercury release from the Mediterranean region is 4.3 Mg for the year 2006. This is about 80% higher than our estimate of 2.3 Mg for the same period. The difference is proportional to the ratio of in carbon emissions from the two estimates. The carbon emission value of Cinnirella et al. (2008) is the result of very low burn areas and high values for fuel burned m[-2] which yield compensated values for carbon emissions. Here is a case where burn areas and fuel burned vary by factors 6-10, while the mercury emissions are within a factor of <2 because the EF(Hg) used are closely similar, 112 versus 104.

Russian Federation: Here the comparison is complicated because burned area (Mha yr^{-1}), fuel burned (kg m^{-2}) vary significantly, and different EF(Hg) have been used. The value given in parenthesis for Conard and Davidenko (1996), 63 Mg, is a calculated value based on the boreal forest EF(Hg) of 345 µg Hg/kg (dm). Recently, Sukhinin et al. (2004) reported a burned area estimate, similar to Conard and Davidenko (1996) for the period 1995-1997. They indicated that their estimate is

still conservative given the shortcomings of a satellite-based approach to observe burned scars. Yet, their estimate is a factor of 2-5 higher than the reports from the Russia Federal Forest Service (RFFS), which Sukhinin et al. (2004) suggested to be an underestimate due to limited regions monitored by RFFS (i.e. there are uncontrolled and undocumented fires in unprotected zones). These regions have been decreasing in recent years due to fire suppression. As mentioned in the previous section, the GFEDv2 burned area is higher than Sukhinin et al. (2004). It is however, significantly lower relative to ground-based and satellite-based estimates by Cinnirella and Pirrone (2006) and climatological estimate by Lavoué et al. (2000). We note that the period of the data comparison is slightly different, and may in part, account for the discrepancies. The rest of the difference can be attributed to differences in fuel burned and EF(Hg)'s, which in some cases, have compensating effects to the estimates in Hg emissions.

China: There is a discrepancy between our and the Streets and al. (2003, 2005) assessments because of a 10 fold difference in burn areas for forest and grassland fires as well as burning of crop residues and agricultural wastes. Here is a case where methodology limitations may play the decisive role: the GFEDv2 model may underestimate significantly the extensive and frequent crop residue fires. However, the burn areas for forest and grassland fires by themselves are also in doubt. Yan et al. (2006) claimed that Streets et al. overestimated burn areas taken from 1950-1992 by a factor of 10. They reported that the burned area in recent decades had decreased dramatically relative to the averaging period (1950-1992) used by Streets et al (2003) (as much as a factor 10) due in part to fire suppression. We note that the bulk of the estimate in carbon as well as in mercury in China is attributed to crop residue burning rather than forest and grassland fires. This highlights the importance of applying appropriate EFs and points out the limitation of GFEDv2 (and other satellite-derived estimates) to detect small-scale biomass burning.

USA: In this case, the inputs for the two studies, GFEDv2 and that used by Wiedinmyer and Friedli (2007), i.e. burn area, fuel burned, are in reasonable agreement and lead to correspondingly reasonable agreements in carbon emissions. Discounting the difference in EF(Hg) used in the two calculations, there is still a factor of two difference in mercury emission, which must be attributed to the model assumption differences, not yet understood. The average mercury emission calculated by the two models are 20.3 and 43 (range 20-65) Mg Hg yr^{-1}, much larger than the 7.2 ± 2.2 Mg Hg yr^{-1} calculated with GFEDv2 model.

Amazon: This is an example where the application of GFEDv2 may be of limited use because of poor fire detection and burn area assessment for small-scale fires, smoke obscuration and incorrect assumptions about fuel consumption. In the slash and burn operations as practiced in the Amazon the amount of fuel burned is much higher, e.g. 10.6 kg m^{-2} as reported by Michelazzo et al. (2008), compared to 5.4 kg m^{-2} mean fuel consumption assumed in the GFEDv2 model for SHSA. The experimental EF(Hg)'s are 61.0 and 50.4 µg Hg kg^{-1} for 2005 and 2004, compared to the 1997-2006 averages of 145-157 µg Hg kg^{-1} estimated for the GFEDv2 model. Earlier estimates for SA slash and burn mercury emissions range from 8.7 to 90 Mg Hg yr^{-1}, compared to our estimate of 108 Mg Hg yr^{-1} for all of NHSA and SHSA.

8.3 Future Work

The highest priority for additional research is the reduction of uncertainties, both in carbon emissions and EF(Hg). In the carbon emission model all uncertainty sources, i.e. fire detection and burn area measurement, inclusion of all affected fuels in all biomes, and combustion completion for all fuels are to be addressed. A specific concern is for regions that are inadequately described in terms of vegetation speciation and fire behaviour, or exhibit unusually large uncertainties. A new opportunity is the inclusion of the fire dynamics data becoming available from satellite measurements (Roberts and Wooster, 2007). Validation with ground based statistics needs to continue, and the advances in remote sensing promise further progress and insights. Emission models are indispensable for unbiased global comparisons, although local areas may not always be correctly represented in a global model.

The EF(Hg) are more poorly defined than carbon emission uncertainties. Refinement in measuring techniques, conceptual understanding, and above all, more regional measurements are needed. Most available data is from Europe and North America, both minor contributors to global mercury emissions from biomass burning. EF(Hg) from the large carbon emitters, NHAF, SHAF, EQAS, SHAM and BOAS, are very sparse or non-existing. New data should include ground and/or plume measurements using ER or EF determinations. One area poorly understood is the effect of fire dynamics on mercury release in different biomes: e.g. mercury speciation in plumes burning in different biomes under flaming and smouldering conditions. A comprehensive biogeochemical model for mercury in forested areas would provide an understanding of the source/sink balance and thus mercury accumulation or loss in an ecosystem. Such models could then be coupled with carbon emission models and become components of an earth system model. It would also be useful to project climate change impacts. The interaction of fire with fuels and the consequences for mercury release must be better understood. This is particularly true because the mercury and carbon distribution is dramatically different among ecosystems. One of major unknowns is the emission expectations for forests with and without large carbon and mercury reservoirs. For Mediterranean vegetation, savannas, grass lands and agricultural waste, the assessment of above ground fuels by remote or ground-based measurements likely is sufficient to includes all fuel involved in mercury emission. By contrast, in temperate and boreal forests, most mercury is contained in organic soils, which dominate the mercury emissions to variable degrees, depending on fire severity. The role of the top few cm of soil in different landscapes is of paramount importance to mercury emission behaviour. Other possible options to obtain EF(Hg) result from the strong research interest and available data on particulate emissions from biomass burning: i.e. PM2.5, total carbon, organic carbon, total particulate matter, which, combined with mercury assays of the particulates, can yield independent EF(Hg). The fate and transport of emitted mercury is difficult to define because of the regionally different injection heights which lead to unique plume trajectories and associated chemistries and deposition. Some case studies for effluents from the major burn regions, e.g. Africa, Southeast Asia or Siberia, would be useful.

8.4   Policy Implications

Mercury in vegetation and organic soils originates largely from the deposition from the global atmospheric pool and thus must be of global concern. The release of mercury from biomass burning is partially under direct human control. Limiting the burning of tropical and boreal forests (EQAS, SHSA, BOAS) would have two beneficial effects: reducing the source of mercury releases to the atmosphere from burning, and maintaining a sink for atmospheric mercury in the vegetation and organic soil. Restricting the global release of anthropogenic mercury over time would reduce the atmospheric and vegetation/soil pools and thus the release potential in case of fires. Warming as a result of climate change will be felt particularly in boreal forests (Randerson et al., 2006), which harbour huge carbon and mercury pools, and may experience more frequent, larger and more severe wildfires.

References

Amiro, B. D., Todd, J. B., Wotton, B. M., Logan, K. A., Fannigan, M. D., Stocks, B. J., Mason, J. A., Martell, D. L. and Hirsch, K. G., 2001. Direct carbon emissions from Canadian forest fires, 1959 – 1999. *Can. J. For. Res.*, 31, 512–525.

Andreae, M.O. and Merlet, P., 2001. Emission of trace gases and aerosols from biomass burning. *Global Biogeochem. Cyc.*, 15 (4): 955–96.

Arellano, A.F., Kasibhatla, P.S., Giglio, L., van der Werf, G.R., Randerson, J.T. and Collatz, G.J., 2005. Time-dependent inversion estimates of global biomass-burning CO emissions using Measurement of Pollution in the Troposphere (MOPITT) measurements, *J. Geophys. Res.*, 111, D09303, doi:10.1029/2005JD006613.

Barbosa, P.M., Stroppiana, D., Grégoire, J.-M. and Pereira, J.M.C., 1999. An assessment of vegetation fire in Africa (1981-1991): Burned areas, burned biomass, and atmospheric emissions, *Global Biogeochem. Cycles.*, 13(4), 933–950.

Berenfield, M.J., Randerson, J.T., McClain, C.R., Feldman, G.C., Los, S.O., Tucker, C.J., Falkowski, P.G., Field, C.B. and Frouin, R., 2001. Biosphere primary production during an ENSO transition*, Science*, 291 (5513), 2594–2597.

Bergamaschi, P., Hein, R., Heimann, M. and Crutzen, P.J., 2000. Inverse modeling of the global CO cycle: 1. Inversion of CO mixing ratios, *J. Geophys. Res.*, 105, 1909–1927.

Bishop, J.K.B. and Rosswo, W.B., 1991. Spatial and temporal variability of global surface solar irradiance, *J. Geophys. Res.*, 96 (C9), 16839–16858.

Biswas, A., Blum J., Keeler, J., 2006. A comparison of methods to estimate mercury emissions during wildfire, *8th International* Congress on Mercury as a Global Pollutant, T-125.

Biswas, A., Blum J., Keeler, J., 2008. Mercury storage in a central Washington forest and release during the 2001 Rex Creel Fire. STOTEN-D-07-011986. In review

Biswas, A., Blum, J.D., Klaue, B., Keeler, G.J., 2007. Release of mercury from Rocky Mountain forest fires. Global Biogeochem. Cycles, 21, GB1002; doi:10.1029/2006GB002696.

Brunke, E.-G., Labuschagne, C. and Slemr, F. Gaseous mercury emissions from a fire in the Cape Peninsula, South Africa, during January 2000, *Geophys. Res. Lett.*, 28, 1483–1486, 2001.

Carvalho, J.J., Costa, F.S., Gurgel Veras, C.A., Sandberg, D.V., Alvarado, E.C., Serra, A.M. and Santos, J.M. Biomass fire consumption and carbon release rates of rainforest-clearing experimens conducted in northern Mato Grosso, Brazil, *J. Geophys. Res.*, 106(16), 17877–17887, 2001.

Cinnirella, S. and Pirrone, N. Spatial and temporal distribution of mercury emissions from forest fires in Mediterranean region and Russian federation. *Atmos. Environ.*, 40, 7346–7361, 2006.

Cinnirella, S., Pirrone, N., Allegrini, A., Guglietta, D., 2008. Modeling mercury emissions from forest fires in the Mediterranean region, *Environmental Fluid Mechanics*, 8: 129–145.

Conard, S.G. and Davidenko, E.P. Fire in Siberian Forests- Implications for global Climate and Air Quality. USDA Forest Service Gen. Tech. Rep.PSW-GTR-166, 87–94, 1996.

Driscoll, C., Bushey, J T., Nallana, A.G., Selvendiran, P., Choi, H.-Y. and Holsen T.M. Atmosphere-Land Dynamics of Mercury in a Forest Landscape of the Adirondack Region Page of New York, http://nadp.sws.uiuc.edu/meetings/fall2007/post/6-mercury/driscoll.pdf

Duncan, B.N., Martin, R.V., Staudt, A.C., Yevich, R. and Logan, J.L. Interannual and seasonal variability of biomass burning emissions constrained by satellite observations, *J. Geophys. Res.*, 108(D2), 4100, doi:10.1029/2002JD002378, 2003.

Ebinghaus, R., Slemr, F., Brenninkmeijer, C.A.M., vanVelthoven, P., Zahn, A., Hermann, M., Sullivan, D.A. and Oram, D.E. Emission of gaseous mercury from biomass burning in South America in 2005 observed during CARIBIC flights, *Geophys. Res. Lett.*, 34, L08813; doi:10.1029/2006GL028866, 2007.

Engle, M.A., Sexauer Gustin, M., Johnson, D.W., Murphy, J.F., Miller, W.W., Walker, R.F., Wright, J., Markee, M. Mercury distribution in two Sierran forest and one desert sagebrush steppe ecosystems and the effects of fire, *Science of the Total Environment*, 367, 222–233, 2006.

Erickson, J.A., Gustin, M.S., Schorran, D.E., Johnson, D.W., Lindberg, S.E. and Coleman, J.S. Accumulation of atmospheric mercury in forest foliage, *Atmos. Environ.*, 37, 1613–1622, 2003.

Fay, L. and Gustin, M. Assessing the influence of different atmospheric and soil mercury concentrations on foliar mercury concentrations in a controlled environment, *Water, Air and Soil Poll.* 181, 373–384, 2007, doi10.1007/s11270-006-9308-6.

French, N.H.F., Goovaerts, P., Kasischke, E. Uncertainty in estimating carbon emissions from boreal forest fires. *J. Geophys. Res.*, 109, D14S08; doi:10.1029/2003JD003635, 2004.

Frescholtz, T.F., Gustin, M.S., Schorran, D.E. and Fernandez, G.C.J. Assessing the source of mercury in foliar tissue of quaking aspen, *Environ. Toxicol. Chem.*, 22(9), 2114–2119, 2003.

Friedli, H.R., Radke, L.F., Payne, N.J., McRae, D.J., Lynham, T.J. and Blake, T.W. Mercury in vegetation and organic soil at an upland boreal forest site in Prince Albert National Park, Saskatchewan, Canada. *J. Geophys. Res.*, 112, G01004; doi:10.1029/2005JG000061, 2007.

Friedli, H.R., Radke, L.F., Lu, J.Y., Banic, C.M., Leaitch, W.R. and MacPherson, J.I. Mercury emissions from burning of biomass from temperate North American forests: Laboratory and airborne measurements, *Atmos. Environ.*, 37, 253–267, 2003a.

Friedli, H.R., Radke, L.F., Prescott, R., Hobbs, P.V. and Sinha, P. Mercury emissions from the August 2001 wildfires in Washington State and an agricultural waste fire in Oregon, and atmospheric mercury budget estimates, *Global Biogeochem. Cycles*, 17(2), 1039, doi:10.1029/2002GB001972, 2003b.

Friedli, H.R., Radke, L.F., Lu, J.Y. Mercury in smoke from biomass fires. *Geophys. Res. Lett.* 28 (17), 3223–3226, 2001.

Friedli, H.R. et al. Mercury emissions from experimental burns of Southern African vegetation, unpublished MS, 2008.

Fromm, M.D. and Servranckx, R. Transport of forest fire smoke above the tropopause by supercell convection, *Geophys. Res. Lett.*, 30(10), 1542, doi:10.1029/2002GL016820, 2003.

Giglio, L., van der Werf, G.R., Randerson, J.T., Giglio, L., Collatz, G.J. and Kasibhatla, P.S. Global estimation of burned area using MODIS active fire observations, *Atmos. Chem. Phys.*, 6, 957–974, 2006.

Grégoire, J.-M., Tansey, K. and Silva, J.M.N. The GBA2000 initiative: Developing a global burned area database from SPOT-VEGETATION imagery, *Int. J. Remote Sensing*, 24(6), 1369–1376, 2002.

Grigal, D.F. Mercury sequestration in forests and peatlands: A review. *J. Environ. Qual.*, 32, 393–405, 2003.

Grigal, D.F. Inputs and output of mercury from terrestrial watersheds: a review. *Environ. Rev.* 10, 1–39, 2002.

Guild, L.S., Kauffman, J.B., Ellingson, L.J., Cummings, D.L., Castro, E.A., Babbitt, R.E. and Ward, D.E. Dynamics associated with total aboveground biomass, C, nutrient pools, and biomass burning of primary forest and pasture in Rondonia, Brazil during SCAR-B, *J. Geophys. Res.*, 103 (D24), 32091–32100, 1998.

Gustin, M.S., Lindberg, S.E., Wesiberg, P. An update of our understanding of the role of sources and sinks of the biogeochemical cycle of mercury, 2008, Applied Geochemistry, in press

Hao, W.M. and Liu, M.H. Spatial and temporal distribution of tropical biomass burning, *Global Biogeochem. Cyc.*, 8(4), 495–503, 1994.

Harden, J.W., Neff, J.C., Sandberg, D.V., Turetsky, M.R., Ottmar, R., Gleixner, G., Fries, T.L. and Manies, K.L. Chemistry of burning the forest floor during the FROSTFIRE experimental burn, interior Alaska,1999. *Global Biogeochem. Cycles*, 18, GB3014; doi: 10.1029/2003GB002194, 2004.

Harris, R.C. et al. Whole-ecosystem study shows rapid fish-mercury response to changes in mercury deposition.www.pnas.org/doi:10.1073/pnas.0704186104, 2007

H·ly, C., Alleaume, S., Swap, R.J., Shugart, H.H. and Justices, C.O. SAFARI-2000 characteristics of fuels, fire behavior, combustion completeness, and emissions from experimental burns in infertile grass savannas in western Zambia, *J. Arid Environ*, 54, 381–394, 2003.

Hobbs, P.V., Reid, J.S., Herring, J.A., Nance, J.D., Weiss, R.E., Ross, J.L., Hegg, D.A., Ottmar, R.D. and Liousse, C. Particles and trace gas measurements in smoke from prescribed burns of forest products in the Pacific Northwest, in Biomass Burning and Global Change, vol 1, edited by J.S. Levine, pp. 697–715, MIT Press, Cambridge, Mass., 1996.

Hoelzemann, J.J., Schultz, M.G., Brasseur, G.P., Granier, C. and Simon, M. Global Wildland Fire Emissions Model (GWEM): Evaluating the use of global area burnt satellite data, *J. Geophys. Res.*, 109(D14S04), doi:10.1029/2003JD003666, 2004.

Hoffa, E.A., Ward, D.E., Olbu, G.J. and Baker, S.P. Emissions of CO_2, CO, and hydrocarbons from fires in diverse African savanna ecosystems, *J. Geophys. Res.*, 104(D11), 13841–13853, 1999.

Ito, A. and Penner, J.E. Global estimates of biomass burning emissions based on satellite imagery for the year 2000, *J. Geophys. Res.*, 109, D14S05, doi:10.1029/2003JD004423, 2004.

Jain, A.K., Tao, Z., Yang, X. and Gillespie, C. Estimates of global biomass burning for reactive greenhouse gases (CO, NMHCs, and NOx) and CO_2, *J. Geophys. Res.*, 111(D06304), doi:10.1029/2005JD006237, 2006.

Kasischke, E.S., Hyer, E.J., Novelli, P.C., Bruhwiler, L.P., French, N.J.F., Sukhinin, A.I., Hewson, J.H. and Stocks, B.J. Influences of boreal fire emissions on Northern Hemisphere atmospheric carbon and carbon monoxide, *Global Biogeochem. Cyc.*, 19, GB1012, doi:10.1029/ 2004GB002300, 2005.

Kasischke, E.S. and Bruhwiler, L. Emissions of carbon dioxide, carbon monoxide, and methane from boreal forest fires in 1998, *J. Geophys. Res.*, 108 (D1), 8146, doi:10.1029/ 2001JD000461, 2002.

Kasischke, E.S. and Penner, J.E. Improving global emissions of atmospheric emissions form biomass burning, *J. Geophys. Res.*, 109 (D14S01), doi:10.1029/2004JD004972, 2004.

Lavoué, D., Liousse, C., Cachier, H., Stocks, B.J., and Goldammer, J.G. Modeling of carbonaceous particles emitted by boreal and temperate wildfires at northern latitudes, *J. Geophys. Res.*, 105, 26871–26890, 2000.

Lindberg, S.E. Forests and the global biogeochemical cycle of mercury, in *Global and Regional Mercury Cycles: Sources, Fluxes and Mass Balances*, NATO-ASI Ser., vol. 21, edited by W. Baeyens, et al., pp. 359–380, Springer, New York, 1996.

Michelazzo, P.A.M; Fostier, A.H; Magarell, G., Santos, J.C., Carvalho, J.A. Jr. Mercury emissions from forest burning in the region of Alta Floresta. Submitted to Sci. Tot. Environ., 2008.

Müller, J-F. and Stavrakou, T. Inversion of CO and NOx emissions using the adjoint of the IMAGES model, *Atmos. Chem. Phys.*, 5, 1157–1186, 2005.

Obrist, D., Moosmueller, H., Schuermann, R., Antony Chen, L.-w, and Kreidenweis, S.M. Particulate_Phase and Gaseous Elementary Mercury Speciation in Biomass Combustion: Controlling Factors and Correlation with Particulate Matter Emission. Environ. Sci. Technol., 10.1021/es071279n, 2007.

Pétron, G., Grainer, C., Khattatov, B., Yudin, V., Lamarque, J-F., Emmons, L., Gille, J. and Edwards, D.P. Monthly CO surface sources inventory based on the 2000-2001 MOPITT satellite data, *Geophys. Res. Lett.*, 31, L21107, doi:10.1029/2004GL020560, 2004.

Pfister, G., Emmons, L.K., Hess, P.G., Honrath, R.E., Lamarque, J.-F., ValMartin, M., Owen, R.C., Avery, M., Browell, E., Holloway, J., Nedelec, P., Purvis, R., Ryerson, T., Sachse, G., and Schlager, H. (2006), Ozone Production from the 2004 North American Boreal Fires, *J. Geophys. Res.*, 111, D24S07, doi:10.1029/2006JD007695.

Potter, C.S., Randerson, J.T., Field, C.B., Matson, P.A., Vitousek, P.M., Mooney, H.A. and Klooster, S.A. Terrestial Ecosystem Production – A process model based on global satellite and surface data, Global Biogeochem. *Cycles*. 7(4), 811–841, 1993.

Randerson, J.T., Liu, H., Flanner, M.G., Chambers, S.G., Jin, Y., Hess, P.G., Pfister, G., Mack, M.C., Treseder, K.K., Welp, L.R., Chapin, F.S., Harden, J.W., Goulden, M.L., Lyons, E., Neff, J.C., Schuur, E.A.G., and Zender, C.S. The impact of boreal forest fire on climate warming, *Science*. 314, 1130–1132. 2006.

Roberts, G. and Wooster, M.J. New perspectives on African biomass burning dynamics. *EOS*, 88 (18), 369–370, 2007.

Streets, D.G., Yarber, K.F., Woo, J-H., Carmichael, G.R. Biomass burning in Asia: annual and seasonal estimates and atmospheric emissions. *Global Biogeochem. Cycles.* 17(4) 1099, 2003.

Streets, D.G., Hao, J., Wu, Y., Jiang, J., Chan, M., Tian, H., Feng, X. Anthropogenic mercury emissions in China. *Atmos. Environ.* 39, 7789–7806, 2005.

Seigneur, C., Vijayaraghavan, K., Lohman, K., Karamchandani, P., Scott, C. Global source attribution for mercury deposition in the United States, *Environ. Sci. Technol.*, 38, 555–569, 2004.

Seiler, W. and Crutzen, P.J. Estimates of gross and net fluxes of carbon between the biosphere and the atmosphere from biomass burning, *Clim. Change*, 2(3), 207–247, 1980.

Shea, R.W., Shea, B.W., Kauffman, J.B., Ward, D.E., Haskins, C.I. and Scholes, M.C. Fuel biomass and combustion factors associated with fires in savanna ecosystem of South Africa and Zambia, *J. Geophys. Res.*, 101 (D19), 23551–23568, 1996.

Sigler, J.M., Lee, X. and Munger, W. Emission and long-range transport of gaseous mercury from a large-scale Canadian boreal forest fire. *Environ. Sci. Technol.*, 37, 4343–4347, 2003.

Simon, M.S., Plummer, S., Fierens, F., Hoelzemann, J.J. and Arino, O. Burnt area detection at global scale using ATSR-2: The GLOBSCAR products and their qualification, J. Geophys. Res., 109 (D14S02), doi:10.1029/2003JD003622, 2004.

Skyllberg, U., Qian, J., Frech, W., Xia, K., and Bleam, W.F. Distribution of mercury, methyl mercury and organic sulfur species in soil, soil solution and stream of a boreal forest catchment. *Biogeochemistry*, 64, 53–76, 2003.

St. Louis, V.L., Rudd, W.M., Kelly, C.A., Hall, B.D. Rolfhus, K.R., Scott, K.J., Lindberg, S.E. and Dong, W. Importance of the forest canopy to fluxes of methyl mercury and total mercury to a boreal ecosystem, *Environ. Sci. Technol.*, 35, 3089–3098, 2001.

Sukhinin, A.I., French, N.H.F., Kasischke, E.S., Hewson, J.H., Soja, A.J., Csiszar, I.A., Hyer, E.J., Loboda, T., Conrad, S.G., Romasko, V.I., Pavlichenko, E.A., Miskiv, S.I. and Slinkina, O.A. AVHRR-based mapping of fires in Russia: New products for fire management and carbon cycle studies, *Rem. Sens. Environ.*, 96(2), 188–201, 2004.

Turetsky, M.R., Harden, J.W., Friedli, H.R., Flannigan, M., Payne, N., Crook, J., Radke, L.F. Wildfires threaten mercury stocks in northern soils. *Geophy. Res. Lett.*, 33, L16403, doi:10.1029/2005GL025595, 2006.

van der Werf, G.R., Randerson, J.T., Giglio, L., Collatz, G.J., Kasibhatla, P.S. and Arellano, A. Interannual variability in biomass burning emissions from 1997 to 2004, *Atmos. Chem. Phys.*, 6, 3423–3441, 2006.

van der Werf, G.R., Randerson, J.T., Collatz, G.J. and Giglio, L. Carbon emissions from fires in tropical and subtropical ecosystems, *Global Change Bio.*, 9(4), 547–562, 2003.

Veiga, M.M., Meech, J.A. and Ornante, N. Mercury pollution from Deforestation. *Nature*, 368, 816–817, 1994.

Wiedinmyer, C., Quayle, B., Geron, C., Belote, A., McKenzie, D., Zhang, X., O'Neill, S. and Wynne, K.K. Estimating emissions from fires in North America for Air Quality Modeling, *Atmos. Environ.*, 40, 3419–3432, 2006.

Wiedinmyer, C. and Friedli, H. Mercury emission estimates from fires: An initial inventory for the United States, *Environ. Sci. Technol.*, 41, 8092–8098, 2007.

Weiss-Penzias, P., Jaffe, D., Swartzendruber, P., Hafner, W., Chand, D. and Prestbo, E. Quantifying Asian and biomass burning sources of mercury using the Hg/CO ratio in pollution plumes observed at the Mount Bachelor Observatory, *Atmos. Environ.*, 41, 4366–4379, 2007.

Witham, C. and Manning, A. Impact of Russian biomass burning on UK air quality, *Atmos. Environ.* 41, 8075–8090, 2007.

Woodruff, L.G., Harden, J.W., Cannon, W.F., Gough, L.P., 2001. Mercury loss from the forest floor during wildland fire. American Geophysical Union, Fall meeting, abstract # B32B-0117.

Yan, X., Ohara, T. and Akimoto, H., 2006. Bottom-up estimate of biomass burning in mainland China, *Atmos. Environ.*, 40, 5262–5273.